Template Polymerization of Conductive Polymer Nanostructures

Charles R. Martin
Department of Chemistry
Colorado State University
Fort Collins, CO 80523

Table of Contents

REPORT DOCUMENTATION PAGE

OMB No. 0704-0188

1. AGENCY USE ONLY (Leave blank)	2. REPORT DATE	3. REPORT TYPE AND DATES COVERED
	April 23, 1996	Interim

4. TITLE AND SUBTITLE

Template Polymerization of Conductive Polymer Nanostructures

5. FUNDING NUMBERS

Contract # N00014-82K-0612

6. AUTHOR(S)

Charles R. Martin

7. PERFORMING ORGANIZATION NAME(S) AND ADDRESS(ES)

Dr. Charles R. Martin
Department of Chemistry
Colorado State University
Fort Collins, CO 80523

8. PERFORMING ORGANIZATION REPORT NUMBER

ONR TECHNICAL REPORT #104

9. SPONSORING/MONITORING AGENCY NAME(S) AND ADDRESS(ES)

Office of Naval Research
800 North Quincy Street
Arlington, VA 22217

10. SPONSORING/MONITORING AGENCY REPORT NUMBER

11. SUPPLEMENTARY NOTES

12a. DISTRIBUTION/AVAILABILITY STATEMENT

Reproduction in whole or part is permitted for any purpose of the United States Government. This document has been approved for public release and sale; its distribution is unlimited.

12b. DISTRIBUTION CODE

13. ABSTRACT *(Maximum 200 words)*

Nanochemistry is an emerging subdiscipline of the chemical and materials sciences that deals with the development of methods for synthesizing nanoscopic particles of a desired material and with scientific investigations of the nanomaterial obtained. Nanomaterials have numerous possible commercial and technological applications including use in electronic, optical and mechanical devices, drug delivery and bioencapsulation. In addition this field poses an important fundamental philosophical question--how do the properties (e.g., electronic, optical, magnetic, etc.) of a nanoscopic particle of a material differ from the analogous properties for a macroscopic sample of the same material?

14. SUBJECT TERMS

nanomaterials, conductive polymers, microtubules, nanochemistry

15. NUMBER OF PAGES

16. PRICE CODE

17. SECURITY CLASSIFICATION OF REPORT	18. SECURITY CLASSIFICATION OF THIS PAGE	19. SECURITY CLASSIFICATION OF ABSTRACT	20. LIMITATION OF ABSTRACT
UNCLASSIFIED	UNCLASSIFIED	UNCLASSIFIED	

OFFICE OF NAVAL RESEARCH

Contract N00014-82K-0612

R&T CODE: 4133032
Robert J. Nowak

TECHNICAL REPORT NO. 104

Template Polymerization of Conductive Polymer Nanostructures

by

Charles R. Martin

Prepared for publication

in

Handbook of Conductive Polymers

Department of Chemistry
Colorado State University
Ft. Collins, CO 80523-1872

April 23, 1996

I. INTRODUCTION.

Nanochemistry is an emerging subdiscipline of the chemical and materials sciences that deals with the development of methods for synthesizing nanoscopic particles of a desired material and with scientific investigations of the nanomaterial obtained.[1-4] Nanomaterials have numerous possible commercial and technological applications including use in electronic, optical and mechanical devices,[3-7] drug-delivery,[8] and bioencapsulation.[9] In addition, this field poses an important fundamental philosophical question - how do the properties (e.g. electronic, optical, magnetic, etc.) of a nanoscopic particle of a material differ from the analogous properties for a macroscopic sample of the same material?

My research group has been exploring a method for preparing nanomaterials called "template-synthesis." (For recent reviews see.[1,2]) This method entails synthesizing the desired material within the pores of a nanoporous membrane. The membranes employed have cylindrical pores of uniform diameter (Figure 1). In essence, we view each of these pores as a beaker in which a piece of the desired material is synthesized. Because of the cylindrical shape of these pores a nanocylinder of the desired material is obtained in each pore (Figure 2). Depending on the material and the chemistry of the pore wall, this nanocylinder may be solid (a fibril) or hollow (a tubule).

The template method has a number of interesting and useful features. First, it is a very general approach; we have used this method to prepare tubules and fibrils composed of electronically conductive polymers,[9-16] metals,[14,17-23] semiconductors,[24] carbons,[25] and other materials. Furthermore, nanostructures with extraordinarily small diameters can be prepared. For example, Wu and Bein have recently used this method to prepare conductive polymer (polyaniline) nanofibrils with diameters of 3 nm (30 Å).[26] It would be

difficult to make nanowires with diameters this small using lithographic methods. In addition, because the pores in the membranes used have monodisperse diameters, analogous monodisperse nanostructures are obtained. Finally, the tubular or fibrillar nanostructures synthesized within the pores can be freed from the template membrane and collected (Figure 2A). Alternatively, an ensemble of nanostructures that protrude from a surface like the bristles of a brush can be obtained (Figure 2B).

We began our template-synthesis work in 1985 by electrochemically synthesizing the electronically conductive polymer polypyrrole within the pores of a nanoporous polycarbonate filtration membrane.[10] Since then, we[9,11-16] and others[26-35] have explored, in some detail, the electrochemical, electronic and optical properties of template synthesized-conductive polymers. I review this work in this chapter. Topics discussed include the membranes used to do template synthesis, the electronic properties of template synthesized conductive polymer fibrils and tubules, and the morphology of the template synthesized conductive polymers.

II. MEMBRANES USED.

A. "Track-Etch" Membranes. A number of companies (e.g. Nuclepore and Poretics) sell micro- and nanoporous polymeric filtration membranes that have been prepared via the "track-etch" method.[36] As shown in Figures 1A and B, these membranes contain cylindrical pores of uniform diameter. The pores are randomly distributed across the membrane surface. Membranes with a wide range of pore diameters (down to 10 nm) and pore densities approaching 10^9 pores per cm^2 are available commercially. The most commonly used material to prepare membranes of this type is polycarbonate; however, a broad range of materials is amenable to the track-etch process.[36]

B. Porous Alumina Membranes. Membranes of this type are prepared electrochemically from aluminum metal.[37] As indicated in Figure 1C, the pores in these membranes are arranged in a regular hexagonal lattice. Pore densities as high as 10^{11} pores per cm^2 can be achieved.[38] While such membranes are sold commercially, only a limited number of pore diameters is available. We have prepared membranes of this type with a broad range of pore diameters.[19,21,22] We have made membranes with pores as small as 5 nm, and we believe that even smaller pores can be prepared.

C. Other Nanoporous Materials. Tonucci et al. have recently described a nanochannel array glass membrane.[39] Membranes of this type containing pores with diameters as small as 33 nm and densities as high as $3x10^{10}$ pores per cm^2 were prepared. Beck, et al. have prepared a new, large pore-diameter zeolite.[40] Wu and Bein have used the pores in these materials as templates to synthesize polyaniline and graphitic nanofibrils.[26,35] Douglas et al. have shown that the nanoscopic pores in a protein derived from a bacterium can be used to transfer an image of these pores to an underlying substrate.[41] Finally, Ozin discusses a wide variety of other nanoporous solids that could be used as template materials.[3]

III. TEMPLATE METHODS.

Most of our work has focused on polypyrrole, poly(3-methylthiophene), and polyaniline. These polymers can be synthesized via oxidative polymerization of the corresponding monomer. This may be accomplished either electrochemically[10,12,42] or by using a chemical oxidizing agent.[43-45] We have adapted both of these approaches so that they can be used to do template synthesis of conductive polymers within the pores of our nanoporous template membranes. The easiest way to do electrochemical template synthesis is to coat a metal film onto one surface of the membrane and then use this film to

electrochemically synthesize the desired polymer within the pores of the membrane.[12] Chemical template synthesis can be accomplished by simply immersing the membrane into a solution of the desired monomer and its oxidizing agent.[9,16,44]

In developing these template synthetic methods, we made an interesting discovery. When these polymers are synthesized (either chemically or electrochemically) within the pores of the track-etched polycarbonate membranes, the polymer preferentially nucleates and grows on the pore walls.[11,14,46] As a result, polymeric tubules are obtained at short polymerization times (Figure 2A). These tubular structures have been quite useful in our fundamental investigations of electronic conductivity in the template-synthesized materials (vide infra). In addition, tubular structures of this type have a number of proposed technological applications.[47] For example, we have shown that capped versions of our tubules can be used for enzyme immobilization.[9]

The reason the polymer preferentially nucleates and grows on the pore walls is straightforward.[14] While the monomers are soluble, the polycationic forms of these polymers are insoluble. Hence, there is a solvophobic component to the interaction between the polymer and the pore wall. There is also, an electrostatic component because the polymers are cationic and there are anionic sites on the pore wall.[14]

Finally, by controlling the polymerization time, conductive polymer tubules with thin walls (short polymerization times) or thick walls (long polymerization times) can be obtained. This point is illustrated by the transmission electron micrographs shown in Figure 3.[44] For polypyrrole, the tubules ultimately "close-up" to form solid fibrils. By controlling the polymerization time we can make hollow polypyrrole tubules or solid fibrils. In

contrast, the polyaniline tubules will not close-up, even at long polymerization times.[44]

IV. ENHANCED CONDUCTIVITY.

The easiest way to measure the conductivities of our template-synthesized fibrils is to leave them in the pores of the template membrane and measure the resistance across the membrane.[11,15] Provided the number and diameter of the fibrils is known, the measured trans-membrane resistance can be used to calculate the conductivity of a single fibril. Conductivity data obtained in this way for polypyrrole fibrils are shown in Figure 4.[15] While the large-diameter fibrils have conductivities comparable to those of bulk samples of polypyrrole (e.g. electrochemically-synthesized films), the conductivity of the smallest-diameter fibrils is over an order of magnitude higher. Similar enhancements in conductivity have been observed for template-synthesized polyaniline[16,44] and poly(3-methylthiophene).[11] Analogous results have been obtained by Granström and Inganäs.[32]

This trans-membrane conductivity method is a two-point measurement. Contact resistance is always a worry with such measurements; indeed, we must apply substantial pressure across the membrane (7×10^3 psi) in order to obtain reproducible resistance data.[15] We have recently developed a method for forming thin films from our template-synthesized nanostructures.[16,44] This has allowed us to make four-point conductivity measurements on these nanomaterials (without applying pressure during the measurement). The thin films are prepared by dissolving the template membrane, collecting the conductive polymer nanofibrils or nanotubules by filtration to form a film across the surface of the filter, and then compacting this film in an IR pellet press.[16,44]

Figure 5 shows scanning electron micrographs of cross-sections of thin films prepared in this way from polyaniline and polypyrrole nanotubules. Note

that because of the high pressure used in the compaction step ($6x10^4$ psi) the tubular structure can no longer be seen in the cross section of the polyaniline film (Figure 5A). In contrast, the tubular structure is still clearly evident in the film prepared from the polypyrrole nanotubules (Figure 5B). That the polypyrrole nanotubules can survive the high pressures used during the film-compaction step is quite remarkable and indicates that these tubules are either very strong or very resilient.

Table I shows four-point conductivity data for films prepared from polyaniline tubes of various diameters.[16,44] In complete agreement with the two-point data (Figure 4), conductivity increases as the diameter of the tubules used to prepare the film decreases. The conductivity for the film prepared from the narrowest tubes is over five times higher than a film prepared, under the same conditions, from bulk polyaniline.[16,44] While conductivities of films prepared from polypyrrole tubules show the same trend (increasing conductivity with decreasing tubule diameter), the conductivities obtained are lower than those obtained by the two-point method because, as Figure 5B clearly shows, these films are not space filling.

V. MOLECULAR AND SUPERMOLECULAR STRUCTURE.

We, and others, have shown that the polymer chains in the template-synthesized materials are preferentially aligned (enhanced supermolecular order) and that these chains contain fewer conjugation-interrupting defects (improved molecular structure).[13,15,16,32,44] These improvements in molecular and supermolecular structure are responsible for the enhancements in conductivity discussed above.

A. Supermolecular Structure - Chain Alignment. We have used X-ray diffraction and polarized infrared absorption spectroscopy (PIRAS) to prove that the template-synthesized materials show enhanced supermolecular

order.[13,15,16,44] PIRAS entails measuring the absorbance by the sample of two orthogonal polarizations of IR radiation.[48,49] In our case, one polarization is perpendicular to the axes of our fibrils ($I_{\perp}$) and the other has a component that is parallel to the fibril axes ($I_{||}$). In general, if $I_{\perp}$ and $I_{||}$ are absorbed to the same extent, the polymer chains show no preferred orientation. Nonequal absorbance indicates that the polymer chains are preferentially aligned. PIRAS data can be quantified by calculating a parameter called the dichroic ratio, R. An R value of unity means no preferential chain alignment. For our studies, an R value less than one means some degree of alignment, and the lower the R, the greater the extent of alignment.[13,15,16,44]

Table II shows typical R data for polypyrrole fibrils synthesized at two temperatures.[15] While the largest-diameter fibrils show no preferential chain alignment, the narrowest fibrils show strong dichroism, indicating that the polymer chains are aligned. The PIRAS and conductivity data tell a consistent story about the template-synthesized fibrils. The narrowest fibrils have higher conductivities (Figure 4) because the polymer chains are strongly aligned (Table II). Furthermore, fibrils synthesized at low temperatures are more conductive (Figure 4) because the extent of chain alignment is higher for the low temperature material (Table II).

Recall from Figure 3 that by controlling the polymerization time we can prepare tubules with very thin walls (Figure 3A) or tubules with thick walls (Figure 3B). By obtaining PIRAS data as a function of polymerization time, we can explore the extent of polymer chain alignment in the layer of conductive polymer that is deposited directly onto the polycarbonate (short polymerization times) and in subsequently-deposited layers (long polymerization times). Figure 6 shows the results of such an experiment. We find that the layer of polypyrrole that is deposited directly on the pore wall is ordered (low dichroic

ratio) but that the extent of order decreases in subsequently-deposited layers (dichroic ratio approaches unity). Analogous results were obtained with polyaniline tubules.[44]

These data show that a template-synthesized conductive polymer fibril or tubule has a layer of ordered polymer chains at its outer surface and that the extent of this chain order decreases toward the center of the nanostructure. This "anatomy" is shown schematically in Figure 7.[50] The narrowest template-synthesized tubules and fibrils have the highest conductivities because they contain proportionately more of the ordered (and less of the disordered) material (Figure 7).

The template-synthesized conductive polymer nanostructures have this interesting anatomy because the polycarbonate template membranes are stretch-oriented during processing.[44] As a result, the polycarbonate chains on the pore walls are aligned. When conductive polymer is grown on these aligned chains, the conductive polymer chains become, likewise, aligned. This concept of using the polymer chains in a prealigned substrate to align conductive polymer chains synthesized on the surface of this substrate has been demonstrated for other systems.[51] The disordered central core results because the order-inducing influence of the pore wall is ultimately lost in subsequently deposited layers. An analogous effect occurs when polypyrrole is electrochemically deposited on electrode surfaces;[52] i.e. the first layer of polymer chains lies parallel to the electrode surface, but this preferential orientation is lost in subsequently-deposited layers.

Finally, it is worth noting that in the two point conductivity method (Figure 4) we measure conductivity in a direction perpendicular to the chain alignment direction. Nevertheless, conductivity is enhanced relative to bulk polypyrrole. MacDiarmid and Epstein observed an analogous enhancement in conductivity

in a direction perpendicular to the chain axis in stretch-oriented polyaniline.[53] If we could obtain a thin film sample in which the axes of all the tubes were aligned, we could measure the conductivity in a direction parallel to the chain axis. In analogy to the MacDiarmid/Epstein data this should yield even higher conductivities and high conduction anisotropies. We are currently attempting to prepare such uniaxial films.

B. Molecular Structure - Extended Conjugation. Defects that interrupt conjugation include sp^3 carbons, carbonyls, and twists and bends in the polymer chain.[15,43,54-56] We have used a variety of methods, including X-ray photoelectron spectroscopy (XPS), and UV/visible/NIR and Fourier transform infrared (FTIR) spectroscopies to identify and quantify defect sites within conductive polymers.[15,43,54-56] Perhaps the most useful of these methods is a new IR-based approach, developed in these laboratories, for probing the conjugation length in polypyrrole.[43] This method is based on theoretical work by Zerbi.[57,58] We have used this method to show that conjugation lengths in our template-synthesized polypyrroles are longer than in conventional polypyrrole.

Tian and Zerbi conducted a theoretical analysis of the vibrational spectra of polypyrrole.[57,58] This theory successfully predicts the number and position of the main IR bands and also predicts how the intensities and position of these bands change with the extent of delocalization along the polymer chains (i.e. with the conjugation length). The bands at 1560 and 1480 cm^{-1} (Figure 8A) are especially affected by changes in the conjugation length. These changes can be most easily visualized by taking the ratio of the integrated absorption intensity of the 1560 cm^{-1} band to the integrated absorption intensity of the 1480 cm^{-1} band; we call this ratio I_{1560}/I_{1480}.[43]

According to Tian and Zerbi's analysis, I_{1560}/I_{1480} is inversely proportional to the extent of delocalization.[57,58] In order to test this prediction

we chemically synthesized a family of polypyrroles that ranged from being relatively defect free, to having high concentrations of defect sites along the polymer chains; and we used various chemical and instrumental methods of analysis to identify and quantify the various defect sites.[43] As might be expected, polymers with high concentrations of defect sites showed low conductivities, and polymers with lower defect concentrations showed the highest conductivities.[43] More importantly, we found that Zerbi's prediction concerning the effect of extent of delocalization on I_{1560}/I_{1480} was correct - polymers with high concentrations of defect sites (short conjugation lengths) showed high values of I_{1560}/I_{1480} whereas polymers with low concentrations of defect sites (long conjugation lengths) showed low values of I_{1560}/I_{1480}.[43]

Figure 8B shows the application of this method to template-synthesized polypyrrole tubules.[1] As per the PIRAS data in Figure 6, FTIR data were obtained at various times during the polymerization of polypyrrole tubules within a template membrane that contained 400 nm-diameter pores. Note that I_{1560}/I_{1480} increases with polymerization time (i.e. with wall thickness). This clearly shows that the layer of polypyrrole that is deposited directly on the pore wall has extended conjugation relative to subsequently-deposited layers. Hence, these data mirror the PIRAS data shown in Figure 6.

Figure 9 shows another application of this method to the template-synthesized materials. We have previously shown that materials synthesized at low temperatures are more conductive (Figure 4). The relative intensities of the ring-stretching bands in Figure 9 show that the low temperature material has longer conjugation lengths. Hence, the higher conductivity in the low temperature material is attributable to both greater chain alignment (PIRAS, Table II) and extended conjugation (FTIR, Figure 9). Finally, the effect of synthesis temperature on conductivity can be explained as follows. We, and

others, have shown that polypyrrole synthesized at low temperature has a longer conjugation length than polypyrrole synthesized at higher temperature.[56] As a result, the low temperature-synthesized material is more conductive. Low temperature-synthesized polypyrroles have extended conjugation because defect-forming reactions have higher activation energies than the desired $\alpha-\alpha$ linking reaction.[56]

These analyses of conductivity and extent of supermolecular and molecular order have led us to an important generalization - alignment of polymer chains (improvement in supermolecular order) typically produces an increase in conjugation length (improvement in molecular-level order). This observation makes sense because in order to align, the polymer chains must be linear (i.e. straight), and linear chains will have fewer kinks and bends that interrupt conjugation. Finally, by improving molecular and supermolecular order in this way, we obtain materials with enhanced electronic conductivities.

VI. CONDUCTION MECHANISM IN THE TEMPLATE-SYNTHESIZED MATERIALS.

How might the unique "anatomy" (Figure 7) of the template-synthesized nanostructures affect the mechanism of electronic conduction in thin films prepared from these materials? We have been exploring this question in a collaboration with Professor H.D. Hochheimer in the Physics Department here at Colorado State University and Dr. P-H. Hor of the Texas Center for Superconductivity.[50,59-63] These investigations (which are very much on-going) entail measurements of both the temperature and pressure dependence of conductivity in thin films prepared from our template-synthesized nanostructures. Preliminary results of the effect of temperature on conductivity are briefly reviewed here.

According to the Mott variable-range hopping (MVRH) model for conduction in solids, the temperature (T) dependence of electronic conductivity (s) is given by

$$s = K_o T^{-1/2} \exp[-(T_o/T)^{1/n}] \qquad (1)$$

where K_o and T_o are constants and n = 4, 3, or 2 for three-dimensional (3D), 2D, and 1D conduction, respectively.[64,65] According to Equation 1, resistance (R) data for conductive polymer films can be analyzed via plots of $\ln(RT^{-1/2})$ vs. $T^{-1/n}$. The dimensionality of conduction can be obtained from the value of n that yields the best linear plot. The Mott temperature parameter, T_o, can be obtained from the slope. T_o is directly proportional to the density of states at the Fermi level and inversely proportional to the localization length. By conducting such analyses at various applied pressures, information about the effect of pressure on extent of delocalization can be obtained.

Figure 10A shows a plot of $\ln(RT^{-1/2})$ vs. $T^{-1/4}$ for a film prepared from 400 nm-diameter polypyrrole tubules.[50] The points are the experimental data, and the solid curve is the least-squares best fit line. The $\ln(RT^{-1/2})$ data for this film show a $T^{-1/4}$ dependence over a temperature range from about 256 to 20 K. These data indicate that 3D MVRH is appropriate for conduction in this film over this temperature range. To prove this point, we ratioed the measured resistance (R_m) to the best-fit resistance (R_f) at each temperature. These data were then plotted as $\ln(R_m/R_f)$ vs. T, and as indicated in Figure 10B, this analysis was done using R_f values calculated using the 3D, 2D and 1D MVRH models. This analysis clearly shows that only the 3D model fits the experimental data for this sample. Identical results (i.e., 3D MVRH) were obtained for films prepared from 400 nm-diameter polyaniline tubules.[50] The 3D model has been shown to be applicable to polypyrrole and polyaniline samples prepared by conventional synthetic methods.[66-68]

Figure 11A shows analogous data for a film prepared from 50 nm-diameter polypyrrole tubules.[50] In this case, the data show a $T^{-1/3}$ dependence, indicating 2D MVRH (see Figure 11B for proof). Identical results (i.e., 2D MVRH) were obtained for films prepared from small-diameter polyaniline tubules.[50] These data show that the dimensionality of conduction can be predictably and reproducibly changed in template-synthesized conductive polymer samples.

Knotek and co-workers investigated the dimensionality of conduction in amorphous semiconductor films.[69,70] When the film was thick (> 400 nm), 3D conduction was observed, while conduction in thinner films was 2D. They suggest that when the film thickness becomes small relative to the hopping distance (thin films), conduction is constrained to 2D. In contrast, when the film thickness is large relative to the hopping distance (thick films), conduction occurs in 3D.

We have used analogous arguments to explain the change in dimensionality of conduction in our materials.[50] As indicated in Figure 7, our nanostructures consist of a highly ordered (and highly conductive) surface skin surrounding a disordered (and lower conductivity) core. Because the small-diameter tubules have a larger proportion of the ordered material (Figure 7A), conduction in the surface layer predominates. Because this surface layer is thin (ca. 5 nm), conduction is constrained to 2D (Figure 11). Epstein et al. observed an analogous 2D conduction process in films composed of polyacetylene fibrils.[71] They suggest that 2D conduction results because only a thin layer at the surface of the fibril is doped.

In contrast, the large diameter tubules have a larger proportion of disordered material (Figure 7B). As a result, conduction in the disordered phase predominates, despite its lower intrinsic conductivity. Because the

disordered layer is thick, conduction can occur in 3D (Figure 10). While this proposed explanation is consistent with the experimental data, it is clear that we have just scratched the surface in our investigations and analyses of conduction in these unique polymeric materials. These preliminary data set the stage, and point the direction, for future research.

VII. CONCLUSIONS.

We have learned that template synthesis provides a route for controlling the extent of molecular and supermolecular order in electronically conductive polymers. This allows us to predictably vary not only the magnitude of the conductivity but also the conduction mechanism within the material. For these reasons, our template-synthesized nanostructures are proving to be useful materials for exploring the fundamentals of the conduction process in conductive polymers. Such investigations are under way in our laboratories and in a number of other labs around the world.

In addition, while I have not been able to discuss it here, these template-synthesized nanostructures have a number of possible technological and commercial applications. For example, we have recently shown that capped versions of our polypyrrole microtubules can be used for enzymatic bioencapsulation to make a new type of microbioreactor.[9] This tubule-based microbioreactor might find applications in biosensors.[30,72,73] In addition, the groups headed by Profs. Inganäs and Granström of the Department of Physics, University of Linköping, have recently shown that the template approach can be used to prepare nanoscopic, polymeric light-emitting diodes.[33]

Finally, as indicated in the introduction, the template approach is a universal method for preparing nanomaterials. We, and others, have shown that this method can be used to make nanotubules and fibrils of polymers, metals, semiconductors, carbons and other materials. This creates the

interesting possibility of prepare nanowires and nanotubules that are composed (in a spatially-controlled fashion) of more than one material. The simplest example is nano-Schottky barrier composed of a nanowire segment of a semiconducting material in contact with a nanowire segment of an appropriate metal. We have recently described template-synthesized devices of this type.[24]

Cylindrical junctions (i.e. concentric tubules of different materials) should also be possible. For example, consider a nanocapacitor that is 50 nm in diameter and consists of an outer tube of conductive polymer, surrounding an inner tube of an insulating plastic (e.g. polystyrene), surrounding a solid nanowire of a second conductive polymer. One of our alumina template membranes (Figure 1 C) could contain 10^{10} of these nanocapacitors per cm^2 of membrane area. Analogous ideas will lead to nanobatteries, nano-fuel cells and nanoelectronic and electro-optical devices. This next generation of work will be one focus of our research efforts well into the 21st century.

VIII. Acknowledgments. First, I would like to acknowledge the invaluable help of my professional colleagues Prof. H.D. Hochheimer of the Department of Physics, Colorado State University, Drs. P-H. Hor and J. Bechtold of the Texas Center for Superconductivity, University of Houston, and Dr. S.W. Tozer of the National High Magnetic Field Laboratory, Florida State University. Second, this work would not have been possible without the efforts of a number of hardworking and highly-motivated graduate students and post docs. They include Vinod P. Menon, Zhihua Cai, Junting Lei, Wenbin Liang, Ranjani V. Parthasarathy, Gabor L. Hornyak, Leon S. Van Dyke, and Reginald M. Penner. Finally, financial support from the Office of Naval Research is also gratefully acknowledged.

IX. References.

(1) Martin, C. R. *Accounts of chemical research* **1995**, *28*, 61-68.

(2) Martin, C. R. *Science* **1994**, *266*, 1961-1966.

(3) Ozin, G. A. *Adv. Mater.* **1992**, *4*, 612-649.

(4) The Nov. 29, 1991 issue of *Science* contains a series of articles and features under the title "Engineering a Small World: From Atomic Manipulation to Microfabrication."

(5) Bate, R. T. *Sci. Amer.* **1988**, *259*, 96-100.

(6) Devoret, M. H.; Esteve, D.; Urbina, C. *Nature* **1992**, *360*, 547-553.

(7) Jewell, J. L.; Harbison, J. P.; Scherer, A. *Sci. Amer.* **1991**, *265*, 86-94.

(8) Gref, R.; Minamitake, Y.; Peracchia, M. T.; Trubetskoy, V.; Torchilin, V.; Langer, R. *Science* **1994**, *263*, 1600-1603.

(9) Parthasarathy, R.; Martin, C. R. *Nature* **1994**, *369*, 298-301.

(10) Penner, R. M.; Martin, C. R. *J. Electrochem.. Soc.* **1986**, *133*, 2206-2207.

(11) Cai, Z.; Martin, C. R. *J. Am. Chem. Soc.* **1989**, *111*, 4138-4139.

(12) Van Dyke, L. S.; Martin, C. R. *Langm.* **1990**, *6*, 1123-1132.

(13) Liang, W.; Martin, C. R. *J. Am. Chem. Soc.* **1990**, *112*, 9666-9668.

(14) Martin, C. R. *Adv. Mater.* **1991**, *3*, 457-459.

(15) Cai, Z.; Lei, J.; Liang, W.; Menon, V.; Martin, C. R. *Chem. Mater.* **1991**, *3*, 960-966.

(16) Martin, C. R.; Parthasarathy, R.; Menon, V. *Synth. Met.* **1993**, *55-57*, 1165-1170.

(17) Penner, R. M.; Martin, C. R. *Anal. Chem.* **1987**, *59*, 2625-2630.

(18) Brumlik, C. J.; Martin, C. R. *J. Am. Chem. Soc.* **1991**, *113*, 3174-3175.

(19) Foss, C. A. J.; Hornyak, G. L.; Stockert, J. A.; Martin, C. R. *J. Phys. Chem.* **1992**, *1992*, 7497-7499.

(20) Brumlik, C. J.; Martin, C. R.; Tokuda, K. *Anal. Chem.* **1992**, *64*, 1201-1203.

(21) Foss, C. A. J.; Hornyak, G. L.; Stockert, J. A.; Martin, C. R. *Adv. Mater.* **1993**, *5*, 135-136.

(22) Foss, C. A. J.; Hornyak, G. L.; Stockert, J. A.; Martin, C. R. *J. Phys. Chem.* **1994**, *98*, 2963-2971.

(23) Brumlik, C. J.; Menon, V. P.; Martin, C. R. *J. Mater. Res.* **1994**, *9*, 1174-1183.

(24) Klein, J. D.; Herrick, R. D. I.; Palmer, D.; Sailor, M. J.; Brumlik, C. J.; Martin, C. R. *Chem. Mater.* **1993**, *5*, 902-904.

(25) Parthasarathy, R. V.; Martin, C. R. *Adv. Mater., in press.*

(26) Wu, C.-G.; Bein, T. *Science* **1994**, *264*, 1757-1759.

(27) Atchison, S. N.; Burford, R. R.; Darragh, T. A.; Tontong, T. *Polym. Int.* **1991**, *26*, 261-266.

(28) Burford, R. P.; Tongtam, T. *J. Mater. Sci.* **1991**, *26*, 3264-3270.

(29) Cahalane, W.; Labes, M. M. *Chem. Mater.* **1989**, *1*, 519.

(30) Czajka, R.; Koopal, C. G. J.; Feiters, M. C.; Gerritsen, J. W.; Nolte, R. J. M.; Van Kempen, H. *Biochem. Bioenerg.* **1992**, *29*, 47-57.

(31) Koopal, C. G. J.; Nolte, R. J. M. *J. Chem. Soc. Chem. Commun.* **1991**, 1691.

(32) Granstrom, M.; Inganas, O. *Synth. Met.* **1993**, *55-57*, 460-465.

(33) Granstrom, M.; Berggren, M.; Inganas, O. *Science* **1995**, *267*, 1479-1481.

(34) Kyotani, T.; Tsai, L.-F.; Tomita, A. *Chem. Mater.* **1995**, in press.

(35) Wu, C.-G.; Bein, T. *Science* **1994**, *266*, 1013-1015.

(36) Fleischer, R. L.; Price, P. B.; Walker, R. M. *Nuclear tracks in solids*; University of California Press: Berkeley, 1975.

(37) Despic, A.; Parkhutik, V. P. In *Modern aspects of electrochemistry*; J. O. Bockris, R. E. White and B. E. Conway, Eds.; Plenum Press: New York, 1989; Vol. 20; Chap. 6.

(38) AlMawiawi, D.; Coombs, N.; Moskovits, M. *J. Appl. Phys.* **1991**, *70*, 4421-4425.

(39) Tonucci, R. J.; Justus, B. L.; Campillo, A. J.; Ford, C. E. *Science* **1992**, *258*, 783-785.

(40) Beck, J. S.; Vartuli, J. C.; Roth, W. J.; Leonowicz, M. E.; Kresge, C. T.; Schmitt, K. D.; Chu, C. T.-W.; Olson, D. H.; Sheppard, E. W.; McCullen, S. B.; Higgins, J. B.; Schlenker, J. L. *J. Am. Chem. Soc.* **1992**, *114*, 10834-10843.

(41) Douglas, K.; Devaud, G.; Clark, N. A. *Science* **1992**, *257*, 642-644.

(42) Penner, R. M.; Van Dyke, L. S.; Martin, C. R. *J. Phys. Chem.* **1988**, *92*, 5274-5282.

(43) Lei, J.; Cai, Z.; Martin, C. R. *Synth. Met.* **1992**, *46*, 53-69.

(44) Parthasarathy, R. V.; Martin, C. R. *Chem. Mater.* **1994**, *6*, 1627-1632.

(45) Lei, J.; Menon, V. P.; Martin, C. R. *Polym. Adv. Tech.* **1992**, *4*, 124-132.

(46) Martin, C. R.; Van Dyke, L. S.; Cai, Z.; Liang, W. *J. Am. Chem. Soc.* **1990**, *112*, 8976-8977.

(47) Pool, R. *Science* **1990**, *247*, 1410.

(48) Monnerie, L. in*Developments in Oriented Polymers*; I.M. Ward, Ed.; Elsevier: London, 1987; Vol. Vol. 2, p. 199.

(49) Zbinden, R. *Infrared Spectroscopy of High Polymers*; Academic Press: NY, 1964, p. 186.

(50) Spatz, J. P.; Lorenz, B.; Weishaupt, K.; Hochheimer, H. D.; Menon, V. P.; Parthasarathy, R. V.; Martin, C. R.; Bechtold, J.; Hor, P.-H. *Phys. Rev. Lett.* **1994**, *50*, 14,888-14,892.

(51) Wittmann, J. C.; Smith, P. *Nature* **1991**, *352*, 414-417.

(52) Cai, Z.; Martin, C. R. *J. Electroanal. Chem.* **1991**, *300*, 35-50.

(53) MacDiarmid, A. G.; Epstein, A. J. *Synth. Met.* **1994**, *65*, 103.

(54) Lei, J.; Liang, W.; Martin, C. R. *Synth. Met.* **1992**, *48*, 301-312.

(55) Lei, J.; Martin, C. R. *Synth. Met.* **1992**, *48*, 331-336.

(56) Liang, W.; Lei, J.; Martin, C. R. *Synth. Met.* **1992**, *52*, 227-239.

(57) Tian, B.; Zerbi, G. *J.Chem. Phys.* **1990**, *92*, 3886.

(58) Tian, B.; Zerbi, G. *J. Chem. Phys.* **1990**, *92*, 3892.

(59) Hochheimer, H. D.; Lorenz, B.; Tozer, S. W.; Menon, V.; Parthasarathy, R.; Martin, C. R.; Bechtold, J.; Hor, P.-H. *Bull. Am. Phys. Soc.* **1995**, *40*, 345.

(60) Spatz, J. P.; Lorenz, B.; Hochheimer, H. D.; Menon, V.; Parthasarathy, R.; Martin, C. R.; Bechtold, J.; Hor, P.-H. *Bull. Am. Phys. Soc.* **1994**, *39*, 622.

(61) Spatz, J. P.; Lorenz, B.; Hochheimer, H. D.; Menon, V.; Parthasarathy, R.; Martin, C. R.; Bechtold, J.; Hor, P.-H. *Bull. Am. Phys. Soc.* **1994**, *39*, 160.

(62) Lorenz, B.; Spatz, J. P.; Hochheimer, H. D.; Menon, V.; Parthasarathy, R.; Martin, C. R.; Bechtold, J.; Hor, P.-H. *Phil. Mag. B* **1995**, *71*, 929-940.

(63) Lorenz, B.; Spatz, J. P.; Hochheimer, H. D.; Menon, V.; Parthasarathy, R.; Martin, C. R. In *High pressure in materials science and geoscience*; J. Kamarad, Z. Arnold and A. Kapicka, Eds.; Proceedings of the 32nd European High Pressure Research Group Conference: Brno, Czech Republic, 1994; p. 73.

(64) Chien, J. C. W. *Polyacetylene*; Academic Press: NY, 1984, pp 485-488.

(65) Mott, N. F.; Davis, E. A. *Electronic processes in noncrystalline materials;* 2nd ed.; Clarendon Press: Oxford, 1979, pp 32-37.

(66) Meikap, A. K.; Das, A.; Chatterjee, S.; Digar, M.; Bhattacharyya, S. N. *Phys. Rev.* **1993**, *B47*, 1340.

(67) Reghu, M.; Cao, Y.; Moses, D.; Heeger, A. J. *Phys. Rev.* **1993**, *B47*, 1758.

(68) Sato, K.; Yamaura, M.; Hagiwara, T.; Murata, K.; Tokumoto, M. *Synth. Met.* **1991**, *40*, 35.

(69) Knotek, M. L.; Pollak, M.; Donovan, T. M.; Kurtzman, H. *Phys. Rev. Lett.* **1973**, *30*, 853.

(70) Knotek, M. L. *Solid State Commun.* **1975**, *17*, 1431.

(71) Epstein, A. J.; Gibson, H. W.; Chailin, P. M.; Clark, W. G.; Gruner, G. *Phys.Rev. Lett.* **1980**, *45*, 1730.

(72) Koopal, C. G. J.; Nolte, R. J. M.; De Ruiter, B. *J. Chem. Soc. Chem. Commun.* **1991**, 1691.

(73) Kuwabata, S.; Martin, C. R. *Anal. Chem.* **1994**, *66*, 2757.

Table I. Conductivity as a function of tubule diameter for films made from template synthesized polyaniline tubules.

Tubule Diameter (nm)	Conductivity (S cm^{-1})
100	50±4
200	14±2
400	9±2

Table II. Dichroic ratios (R) for polypyrrole fibrils synthesized at two temperatures.

Diameter (nm)	R	
	0° C	25° C
600	--	1.01±0.04
400	0.95±0.04	0.97
50	0.40	0.61
30	0.11	0.17

Figure Captions

Figure 1. Electron micrographs of polycarbonate (**A** and **B**, upper) and alumina (**C** and **D**, lower) template membranes. For each type of membrane, an image of a larger pore membrane is presented (**A** and **C**, left) so that the characteristics of the pores can be clearly seen. An image of a membrane with extremely small pores is also presented (**B** and **D**, right). **A.** Scanning electron micrograph of the surface of a polycarbonate membrane with 1 μm-diameter pores. **B**. Transmission electron micrograph (TEM) of a graphite replica of the surface of a polycarbonate membrane with ca. 30 nm-diameter pores. The pores appear "ragged." This is an artifact of the graphite replica. **C** and **D.** TEM's of microtomed section of alumina membranes with ca. 70 nm (**C**) and ca. 10 nm (**D**)-diameter pores.

Figure 2. **A** (left). Transmission electron micrograph of three polypyrrole nanotubules. **B** (right). Scanning electron micrograph of an array of capped polypyrrole microtubules.

Figure 3. Transmission electron micrographs of thin sections of a polycarbonate membrane during the template synthesis of polyaniline. Polymerization time was 30 min (**A**, upper) and 6 hr (**B,** lower). Note thickness of polyaniline layer on pore walls in **A** vs. **B**.

Figure 4. Conductivity of template synthesized polypyrrole tubules vs. diameter of the tubules. Data for two different synthesis temperatures are shown.

Figure 5. Scanning electron micrographs of cross sections of films made from template-synthesized conductive polymer tubules. **A** (upper). Polyaniline tubules. **B** (lower). Polypyrrole tubules.

Figure 6. Dichroic ratio for polypyrrole tubules (synthesized in a polycarbonate membrane with 400 nm-diameter pores) as a function of polymerization time. Since polymerization time controls tubule wall thickness (see Figure 3) the x-axis is also a wall thickness axis. The band at 1560 cm^{-1} (see Figure 8A) was used to obtain the data.

Figure 7. Anatomy of the polypyrrole tubules. (A) Small and (B) Large outside diameters.

Figure 8. A. IR spectrum of polypyrrole showing the 1560 cm^{-1} (A) and 1480 cm^{-1} (B) bands. **B.** Plot of I_{1560}/I_{1480} vs. polymerization time. Since polymerization time controls tubule wall thickness (see Figure 3) the x-axis is also a wall thickness axis. Membrane as per Figure 6.

Figure 9. FTIR data for 30 nm-dia. polypyrrole fibrils synthesized at three temperatures. Bands at 1560 cm^{-1} and 1480 cm^{-1} are highlighted.

Figure 10. **A** (upper). Resistance data for films prepared from 400 nm-diameter polypyrrole tubules plotted as per 3D MVRH. **B** (lower). Residual analysis showing that only the 3D model fits the data.

Figure 11. **A** (upper). Resistance data for films prepared from 50 nm-diameter polypyrrole tubules plotted as per 2D MVRH. **B** (lower). Residual analysis showing that only the 2D model fits the data.

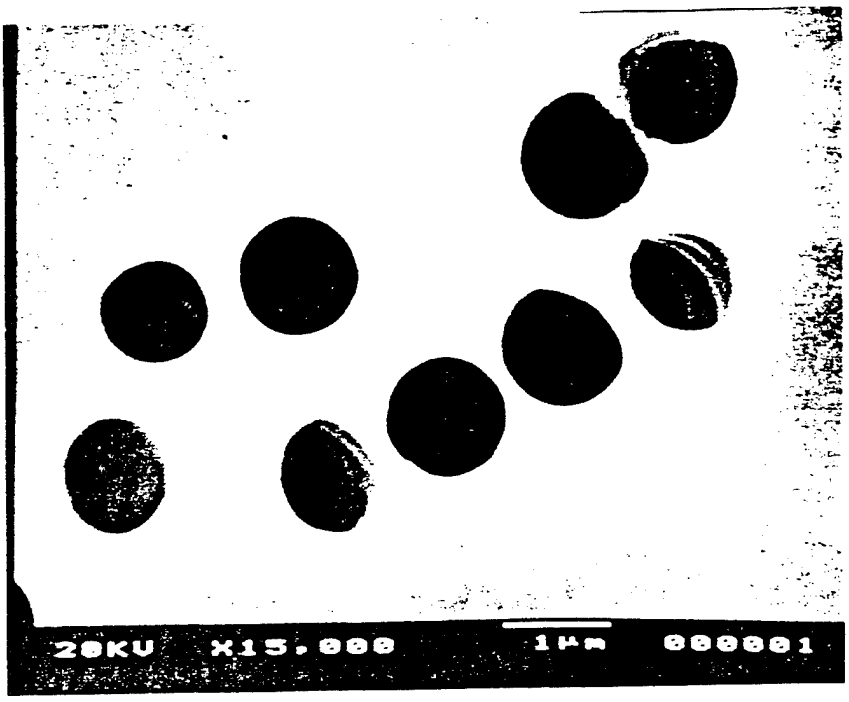
20KV X15,000 1μm 000001


500A PC
114025 80.0KV X40K 200nm

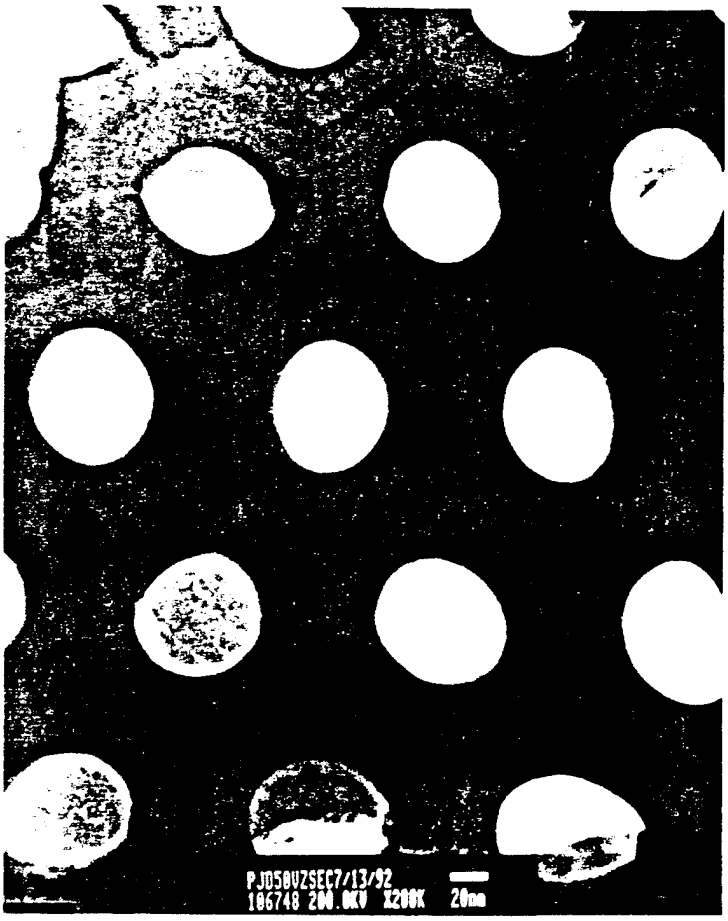
PJD50UZSEC7/13/92
106748 200.0KV X200K 20nm

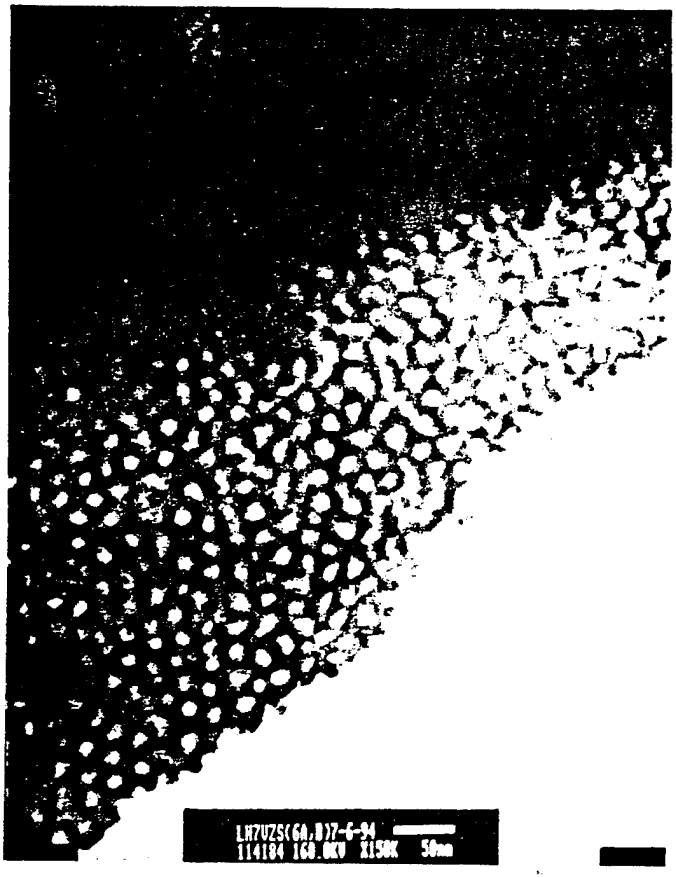
LH7UZS(6A,D)7-6-94
114184 160.0KV X150K 50nm

Fig. 1


0.05 MICRONS PPY
112322 100.0KV X120K 50nm


10µm30.0kV 500E3 0102/06 SCOTCHU

Fig. 2

A.

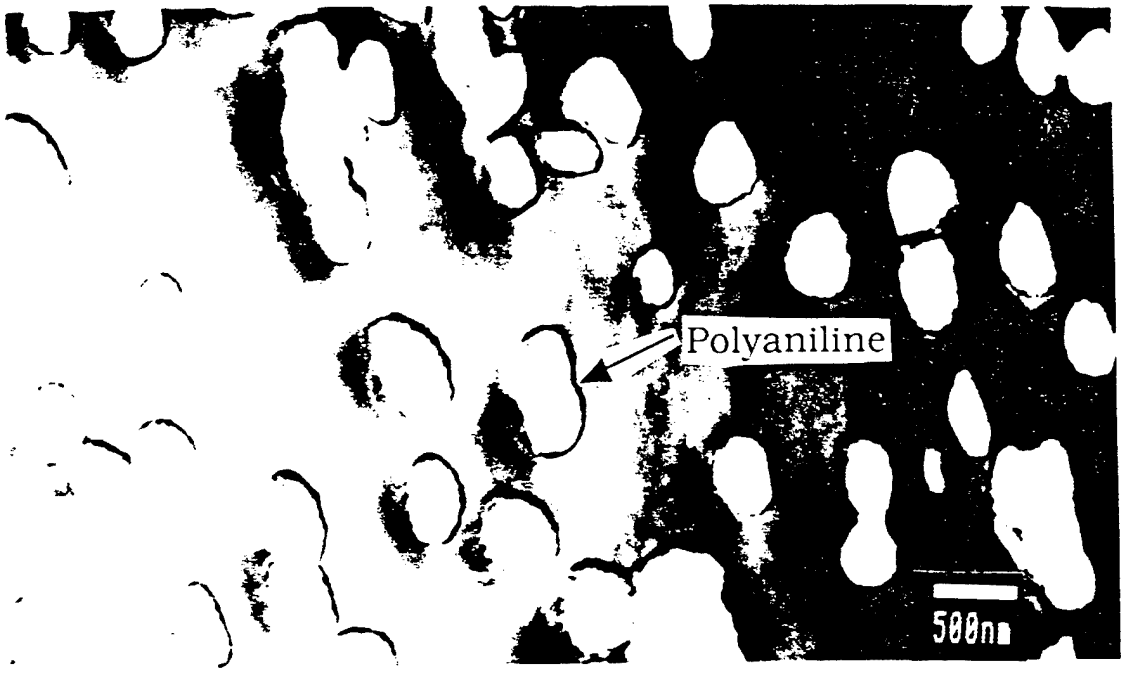

B.

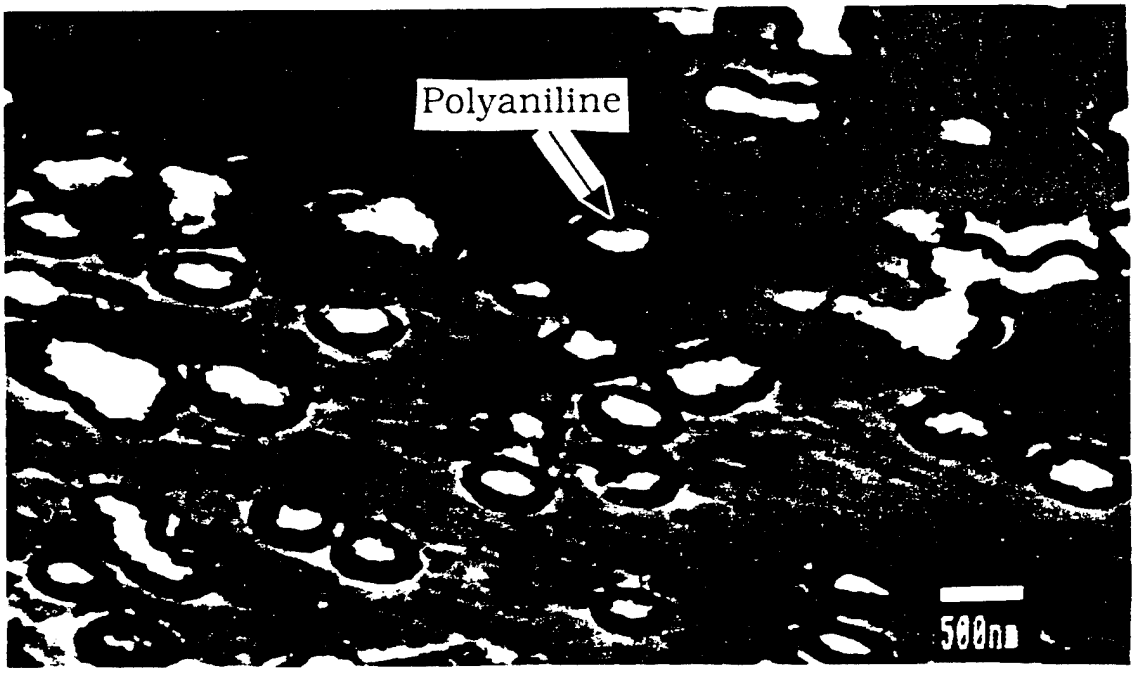

Fig 3

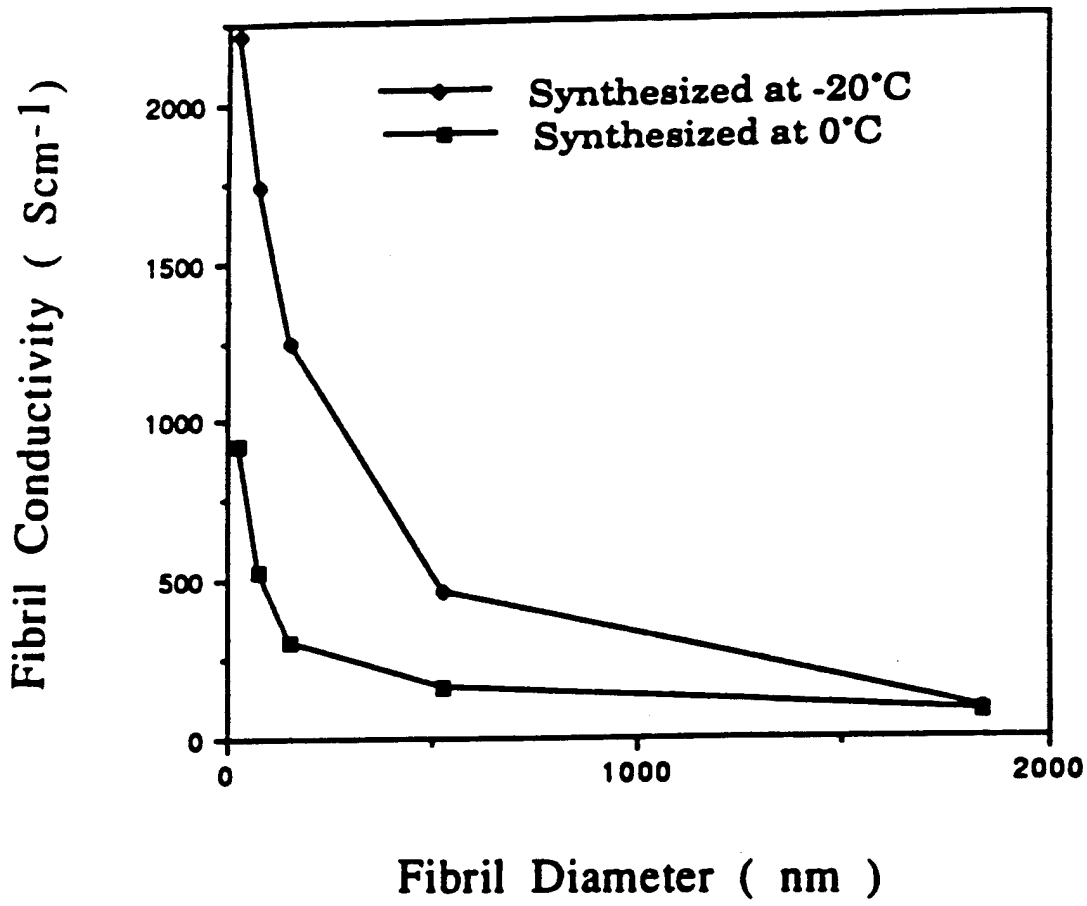
Synthesized at -20°C
Synthesized at 0°C
Fibril Conductivity (Scm-1)
2000
1500
1000
500
0
0
1000
2000
Fibril Diameter (nm)

Fig 4

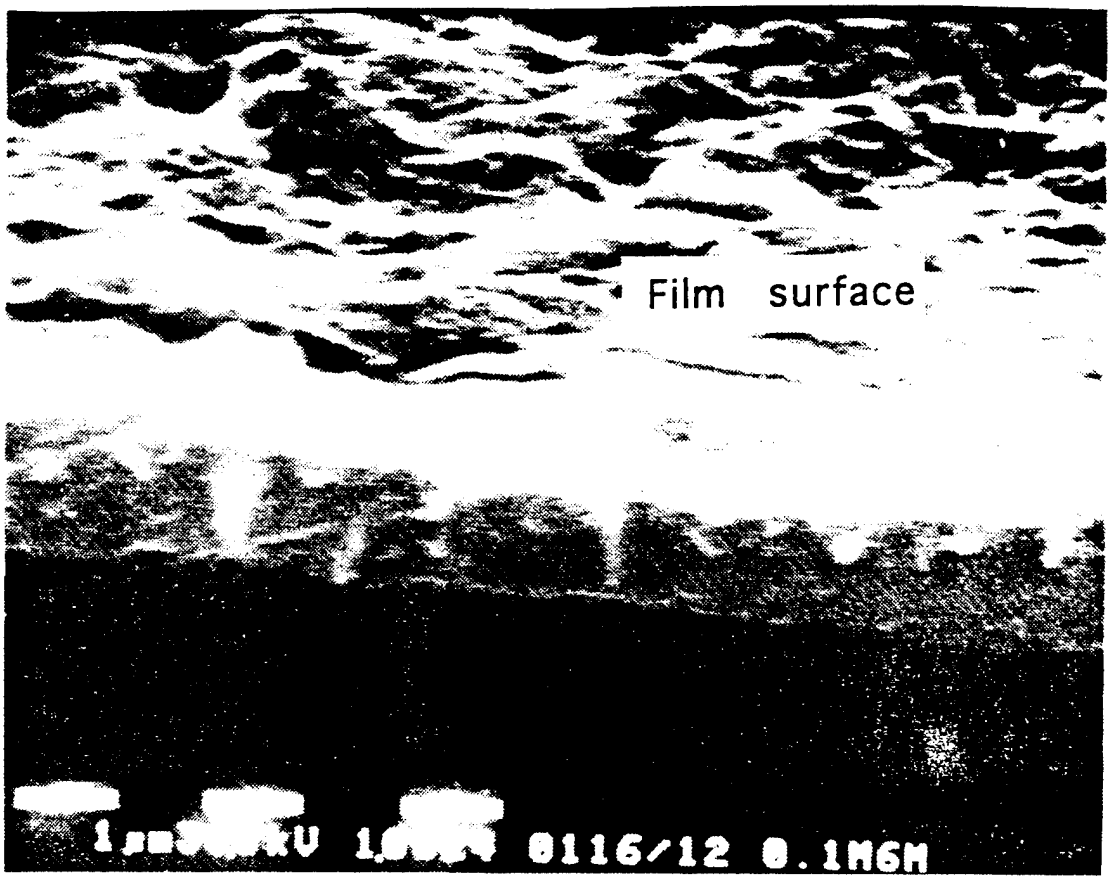
Film surface
Film edge
0116/12 0.1M6M

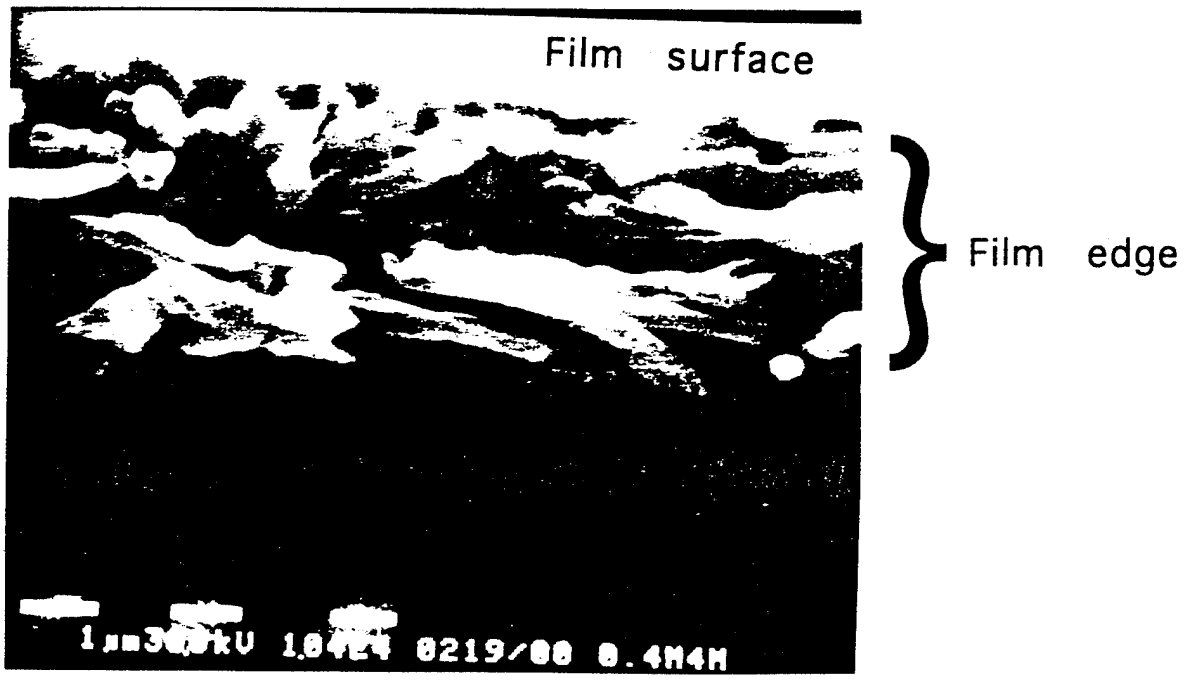
Film surface
Film edge
0219/00 0.4M4M

Fig 5

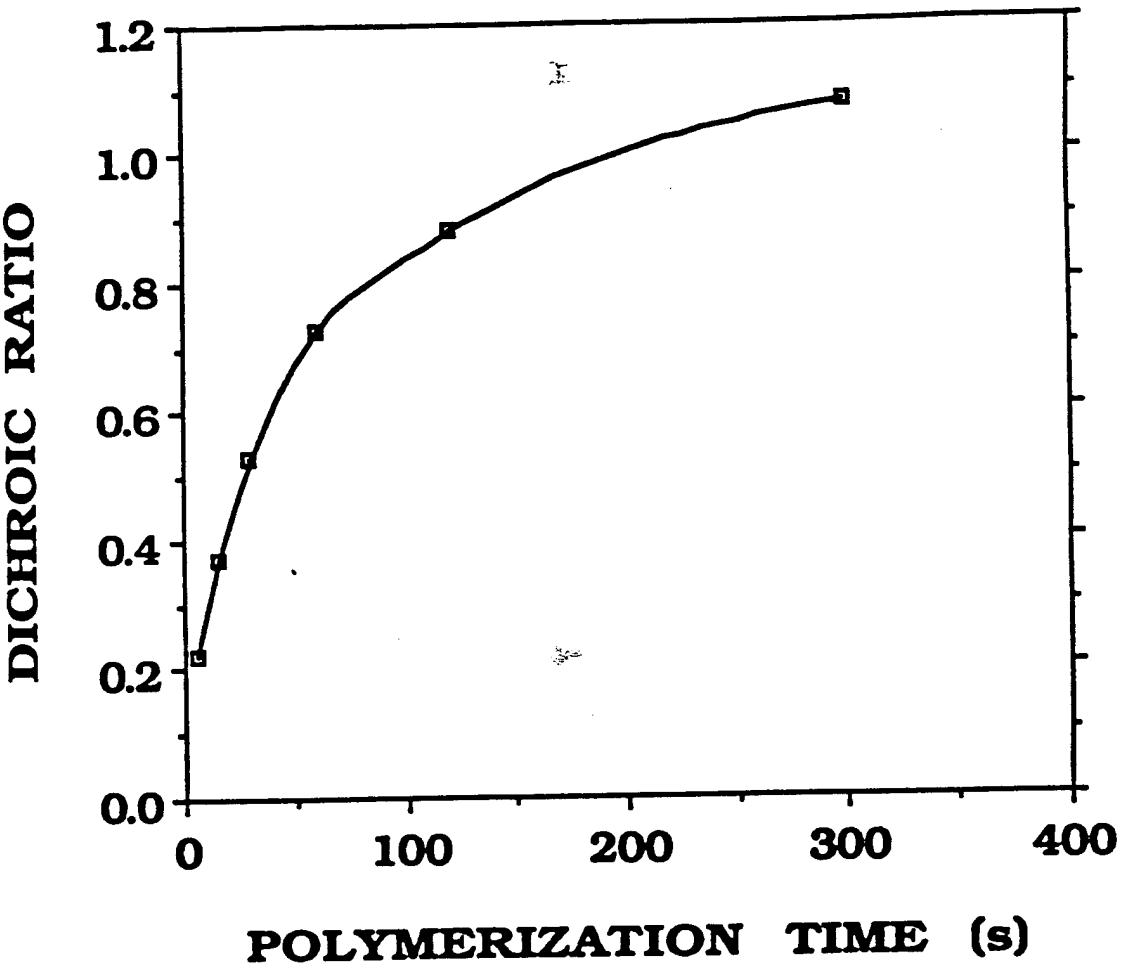
DICHROIC RATIO
1.2
1.0
0.8
0.6
0.4
0.2
0.0
0
100
200
300
400
POLYMERIZATION TIME (s)

Fig. 6

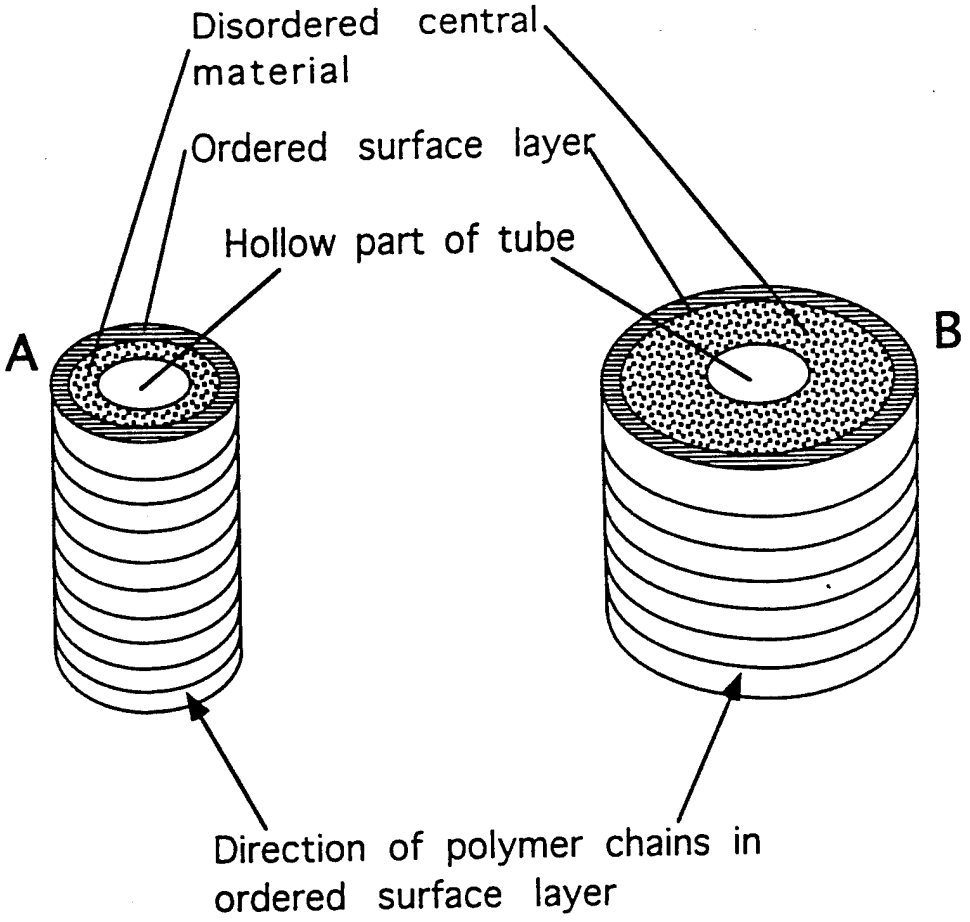
Disordered central material
Ordered surface layer
Hollow part of tube
A
B
Direction of polymer chains in ordered surface layer

Fig 7

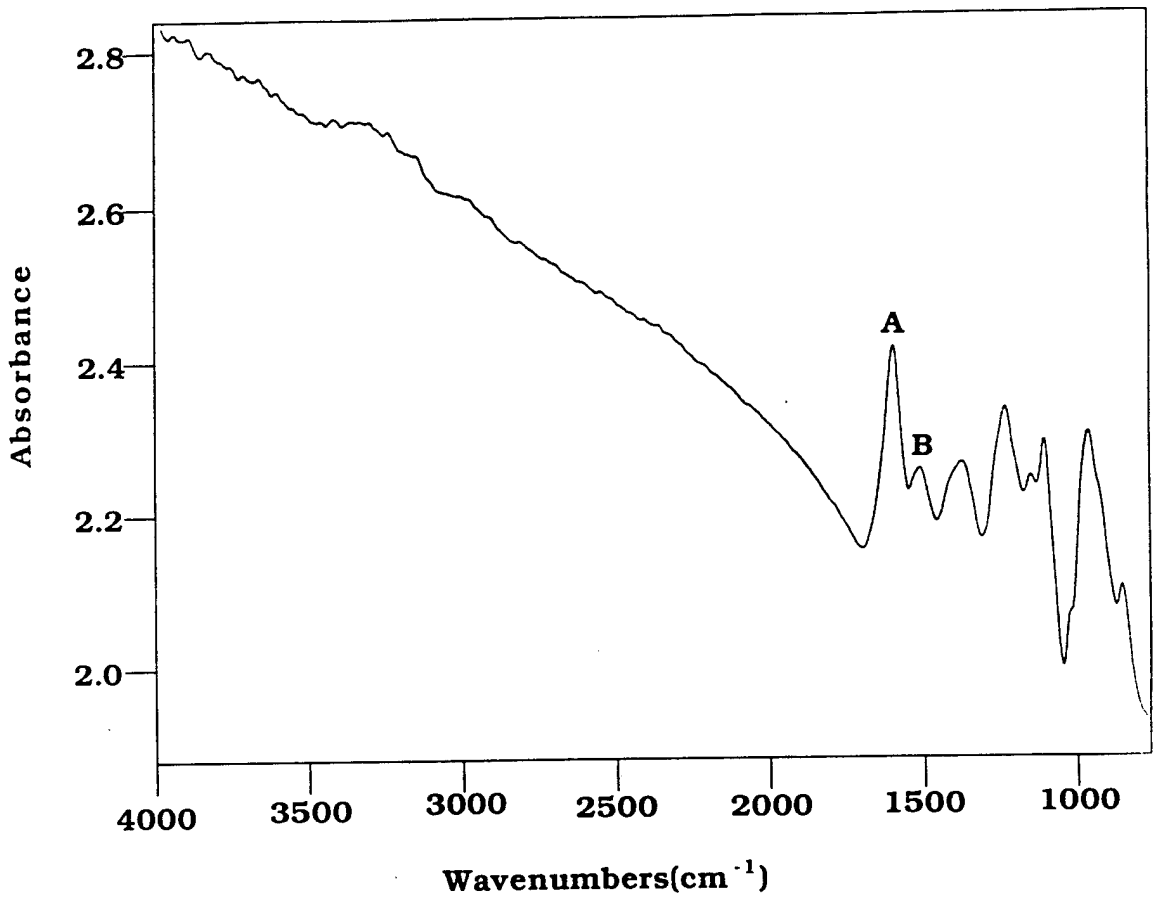
2.8
2.6
2.4
2.2
2.0
Absorbance
A
B
4000
3500
3000
2500
2000
1500
1000
Wavenumbers(cm -1)

Fig 8A

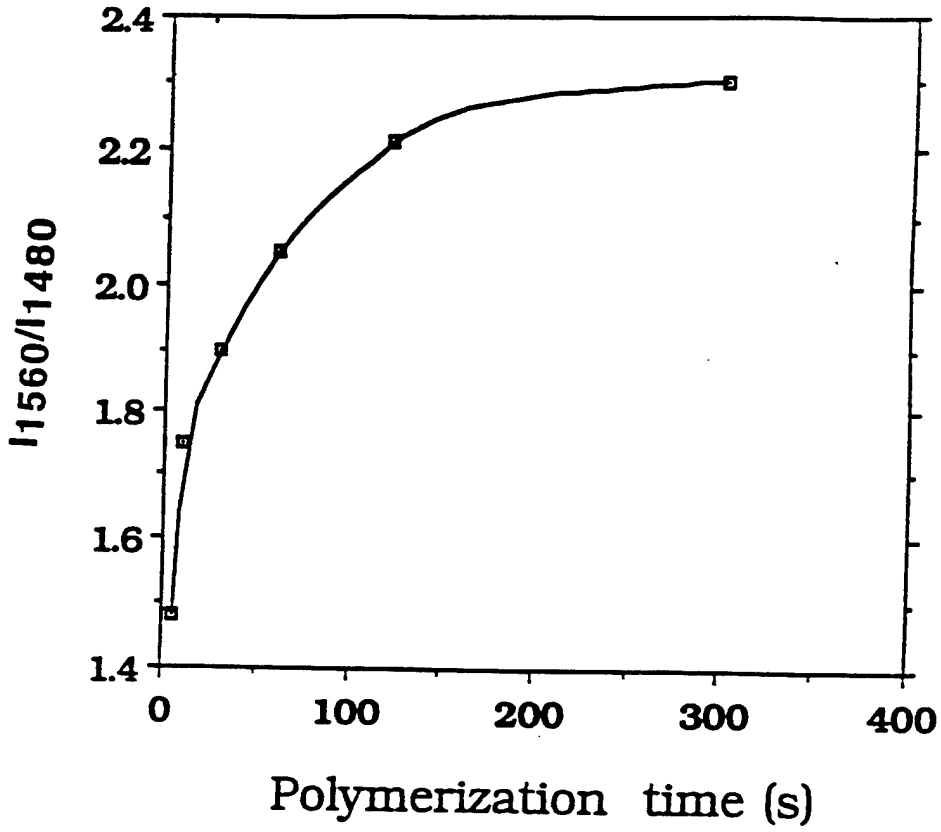
2.4
2.2
2.0
1.8
1.6
1.4
I_{1560}/I_{1480}
0
100
200
300
400
Polymerization time (s)

Fig 8B

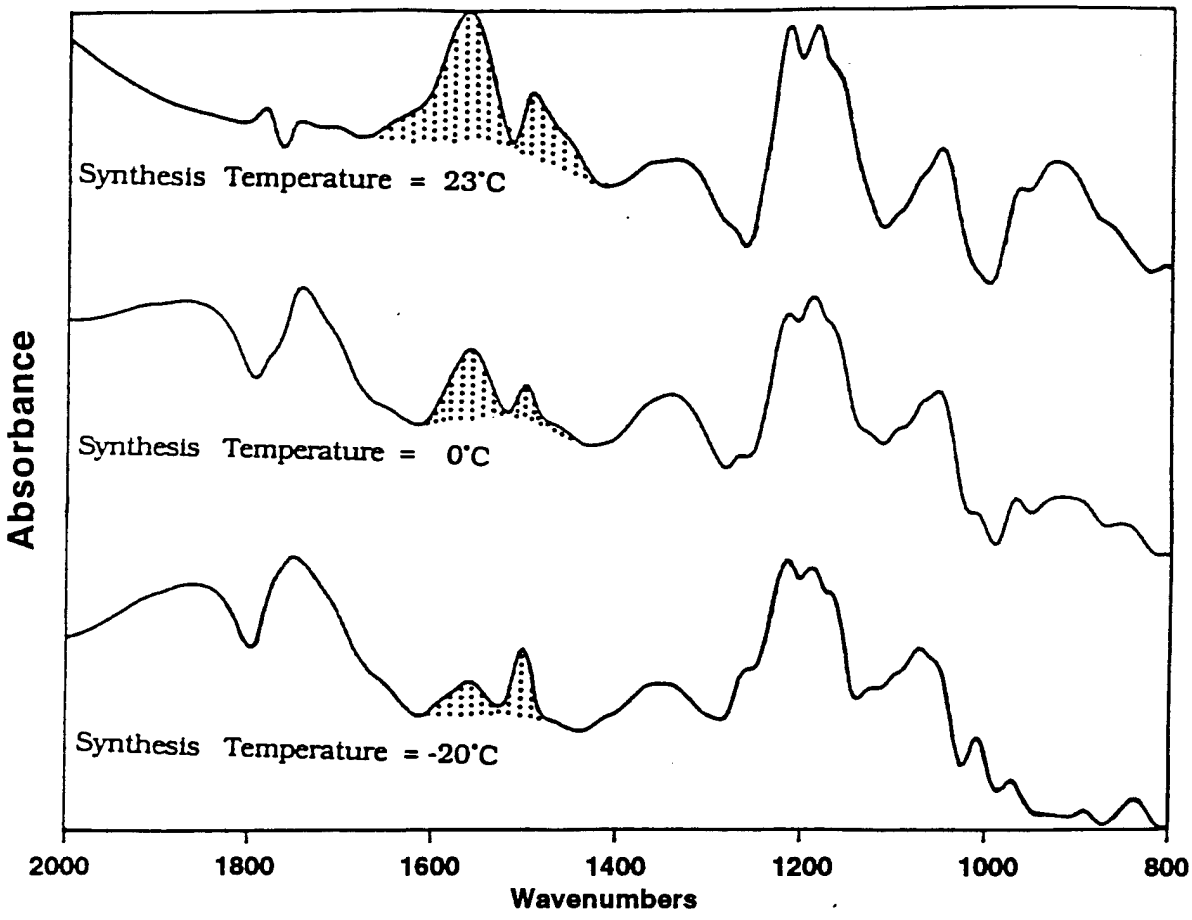
Synthesis Temperature = 23°C
Synthesis Temperature = 0°C
Synthesis Temperature = -20°C
Absorbance
2000
1800
1600
1400
1200
1000
800
Wavenumbers

Fig 9

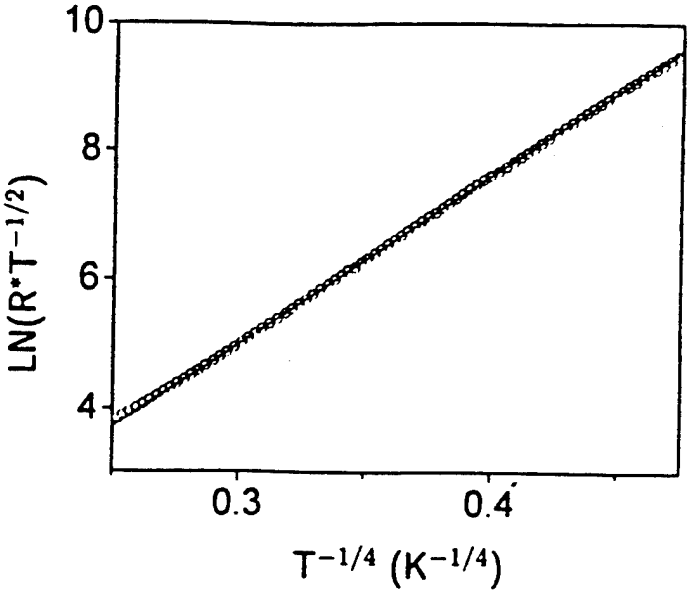

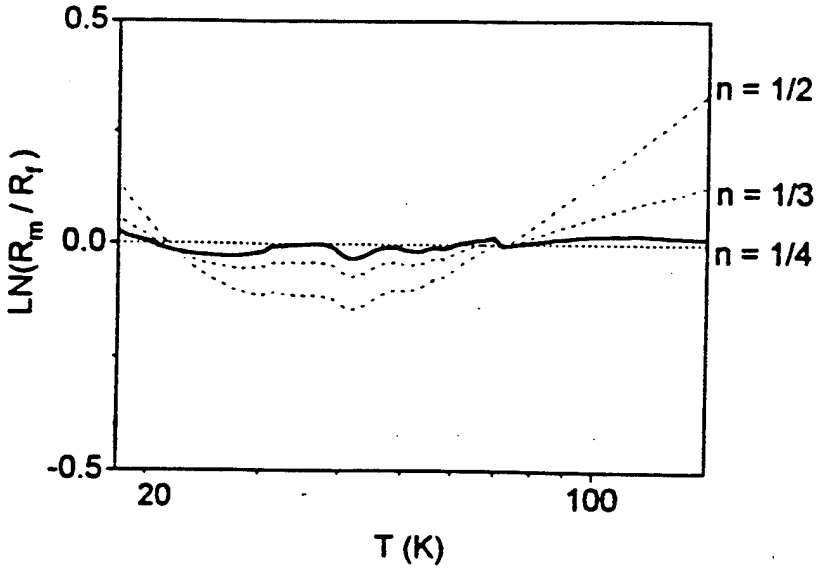

Fig 10

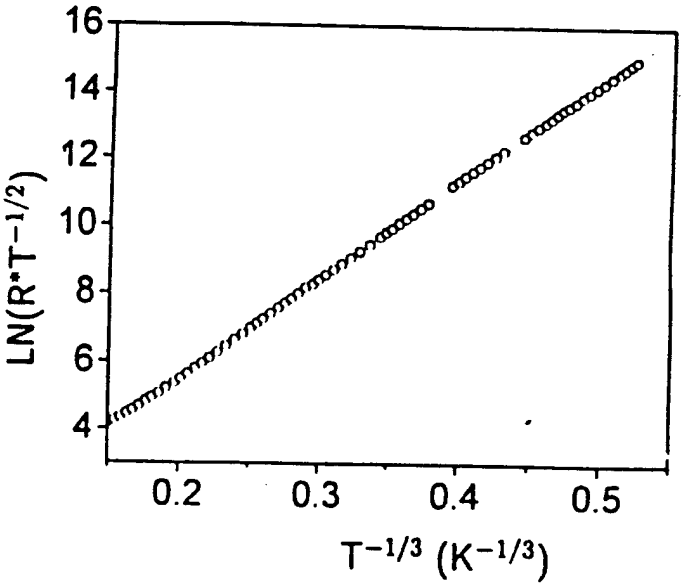
16
14
12
10
8
6
4
LN(R*T^-1/2)
0.2
0.3
0.4
0.5
T^-1/3 (K^-1/3)

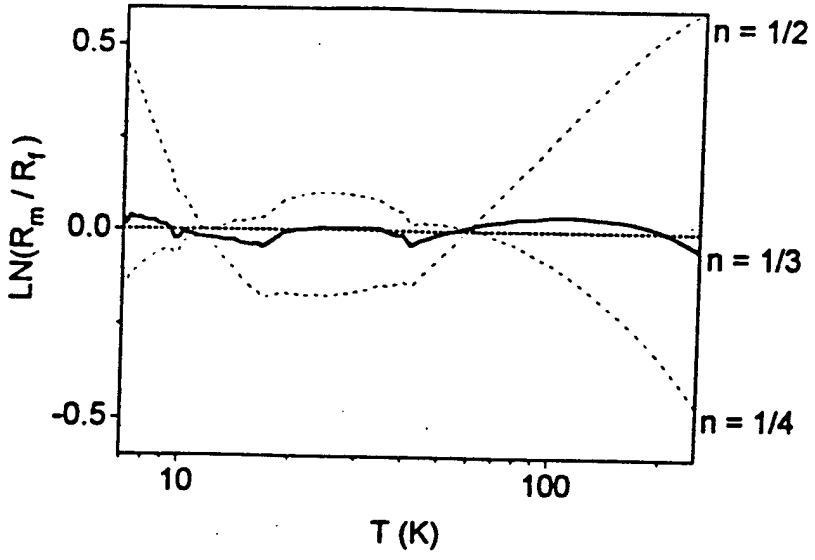
0.5
0.0
-0.5
LN(R_m / R_f)
n = 1/2
n = 1/3
n = 1/4
10
100
T (K)

Fig 11